Copyright WILEY-VCH Verlag GmbH & Co. KGaA, 69469 Weinheim, Germany, 2014.

ADVANCED MATERIALS

Supporting Information

for *Adv. Mater.,* DOI: 10.1002/adma.201401246

Scalable Nanopillar Arrays with Layer-by-Layer Patterned Overt and Covert Images

Kyoung G. Lee, Bong Gill Choi, Byeong Il Kim, Terry Shyu, Myung Seok Oh, Sung Gap Im, Sung-Jin Chang, Tae Jae Lee, Nicholas A. Kotov, and Seok Jae Lee**

Supporting Information

Additional Methods :

Materials: Both UV polymerizable NOA63 (Norland Optic Adhesives) and PU (MINS-311RM, Minuta Tech.) [S1] blend was used to transfer the nanostructures from the molds. The cyclo-olefin copolymer (COC) plate was fabricated using the microinjection mold method as previously reported.[S2] PET film (MITSUBISHI, Japan), clean paper (NanoTech, Republic of Korea), slide glass (Marinenfeld, Germany), fabric (Korea Manufacturer, Korea), and Al foil (DAIHAN, Republic of Korea) were purchased and used without any further processing. 3,3,4,4,5,5,6,6,7,7,8,8,9,9,10,10,10-heptadecafluorodecyl methacrylate (HDFDMA, 97%), *tert*-butyl peroxide (TBPO, 98%), poly(diallyldimethylammonium) chloride (PDDA, 20 wt% in water) and poly(sodium 4-styrenesulfonate) (PSS, MW 70,000) were purchased from Sigma-Aldrich and used without further purification for iCVD.

Fabrication of Si Master Mold: Si wafers were placed in the furnace (Furnace E1200, Centrotherm, Germany) to form a 500 nm thick layer of SiO_2. The thermal oxidized wafer was spin-coated 0.7 μm of photoresist and 500 nm dots were patterned using KrF scanner (S203-B, Nikon, Japan). Following those steps, the Si wafer was etched using ICP (TCP9400SE, Lam Research, USA) and gas mixtures of Cl_2, HBr, and O_2 to produce Si nanopillars. The variety of dimensions of Si nanopillars can be obtained by controlling the oxidation time and etching conditions following from previously reports.[S3,S4] As previously reported, about 46% of Si surface is oxidized due to the stoichiometric ratios and the density difference of Si and SiO_2 [S2]. The overall processes are demonstrated in Fig. S2 and S3.

First Replication from the Master Mold: The conventional casting method with PUNO was employed to create negatives of master mold. First, PUNO was poured and spin-coated on the Si nanopillar and PET film was attached on the top. After carefully rolling over the PET surface to remove air bubbles, the PUNO/PET film was exposed to UV light for 1 min to cure

PUNO as well as increase the adhesion to the film. Subsequently, the PUNO/PET film was peeled off from the Si master mold. For the further curing of PUNO, the film was exposed to UV light for another 5 min.

Formation of Nanopillars on the Substrates: The replication and transfer steps are similar to the above nanohole formation processes. For the fabrication of nanopillars on the target substrates, a previous nanohole array on PET film was used as a secondary mold. PUNO was spin-coated on the nanoholes at 1500 rpm for 30 sec. After PUNO coating, the entrapped air bubbles in PUNO were removed in the vacuum chamber. The target substrates such as PET film, COC, glass, paper, Al foil, and fabric were carefully placed over PUNO. Subsequent rolling of substrate was performed to remove air bubbles and then exposed to UV light for 1 min. After release of the PUNO and target substrate composite from the mold, it was placed under UV light for 5 min. The detailed processes are shown in Fig. S2.

Creating superhydrophilic surface: The surface characteristics of pristine polymeric nanopillars on the different substrates were converted into superhydrophilic surface through SiO_2 coating. The PUNO NPAs were simply loaded into the chamber and SiO_2 was physically sputtered to the surface using multi target plasma sputtering (SRN-110, Sorona, Korea).

Creating superhydrophobic surface through deposition of iCVD polymer: A poly(3,3,4,4,5,5,6,6,7,7,8,8,9,9,10,10,10-heptadecafluorodecyl methacrylate) (pHDFDMA) layer was coated on the surface of fabricated polymeric nanopillars using a customized iCVD reactor (Daeki Hi-Tech Co., Ltd). TBPO was used for an initiator for polymerization of HDFDMA. The vaporized monomer and the initiator, each with a flow rate of 1 sccm, were administered into the iCVD chamber. In order to obtain the target flow rate, TBPO was kept at RT, and HDFDMA was heated to 80 ^{o}C before application into the iCVD reactor. The pressure inside the chamber was set at 80 mTorr. The temperature of the filament was maintained at 210 ^{o}C, while the substrate temperature was set at 37 ^{o}C. The initiator molecules were activated through contact with the heated filament to create radicals. The

radicals transformed the monomer molecules into monomer radicals, which then induced the chain reaction. The radical polymerization reaction continued to take place on the surface of the substrate until the reaction was stopped by turning off the filament and halting the flow of monomer and initiator. The thickness of the coated polymer layer was assessed in situ by He-Ne laser (JDS Uniphase).

Rubbing test: The nanopillar array was fixed on the plastic substrate and rubbed with different types of materials including brush, fabric, and polymeric tips more than 500 times and measured CA and average values were used for the plots.

Process of inkjet LBL deposition: Similar to the previously reported process [S5], high molecular weight PDDA and PSS were diluted to 0.0025 wt% in deionized water as the positive and negative polyelectrolytes, respectively. The patterns were printed using FUJIFILM-Dimatix inkjet printer and alternating cartridges (10 pL drop volume) containing the solutions of PDDA and PSS. Jetting conditions were optimized by adjusting the drive voltage-time waveform for the piezoelectric print-head to produce stable drops. Four bilayers of ink were printed and dried at 35 °C in between prints for 2 min on the printer plate, followed by drying on a hotplate for 1 h after the printing steps.

Characterization of nanopillar arrays: Scanning electron microscopy (SEM, Sirion, FEI), transmission electron microscopy (TEM, JEM 2100-F, 200 kV, JEOL), and energy dispersive X-ray spectroscopy (EDAX) were employed for further analysis of nanostructures and their components. Raman spectra were measured using NTEGRA Spectra spectrometer (NT-MDT, Russia). Changes of surface roughness of nanopillars after SiO_2 coating were investigated using an atomic force microscope (AFM, XE-100, Park Systems, Korea).

Supplementary Data and Figures:

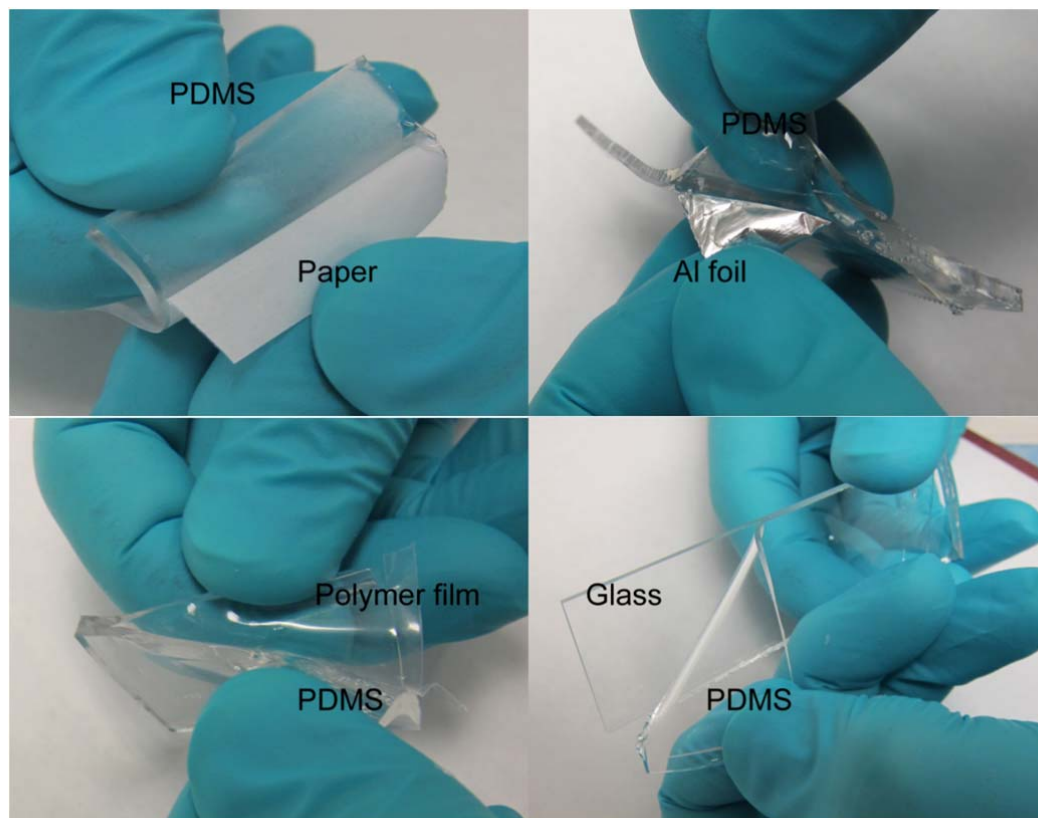

Figure S1. Photographs results of adhesion test between PDMS and other substrates including paper, Al foil, polymer film, and glass, respectively.

The poor adhesion between PDMS mentioned substrates was observed. PDMS normally required extra surface modification to enhance bonding ability with other inorganic or organic substrates.[S6, S7]

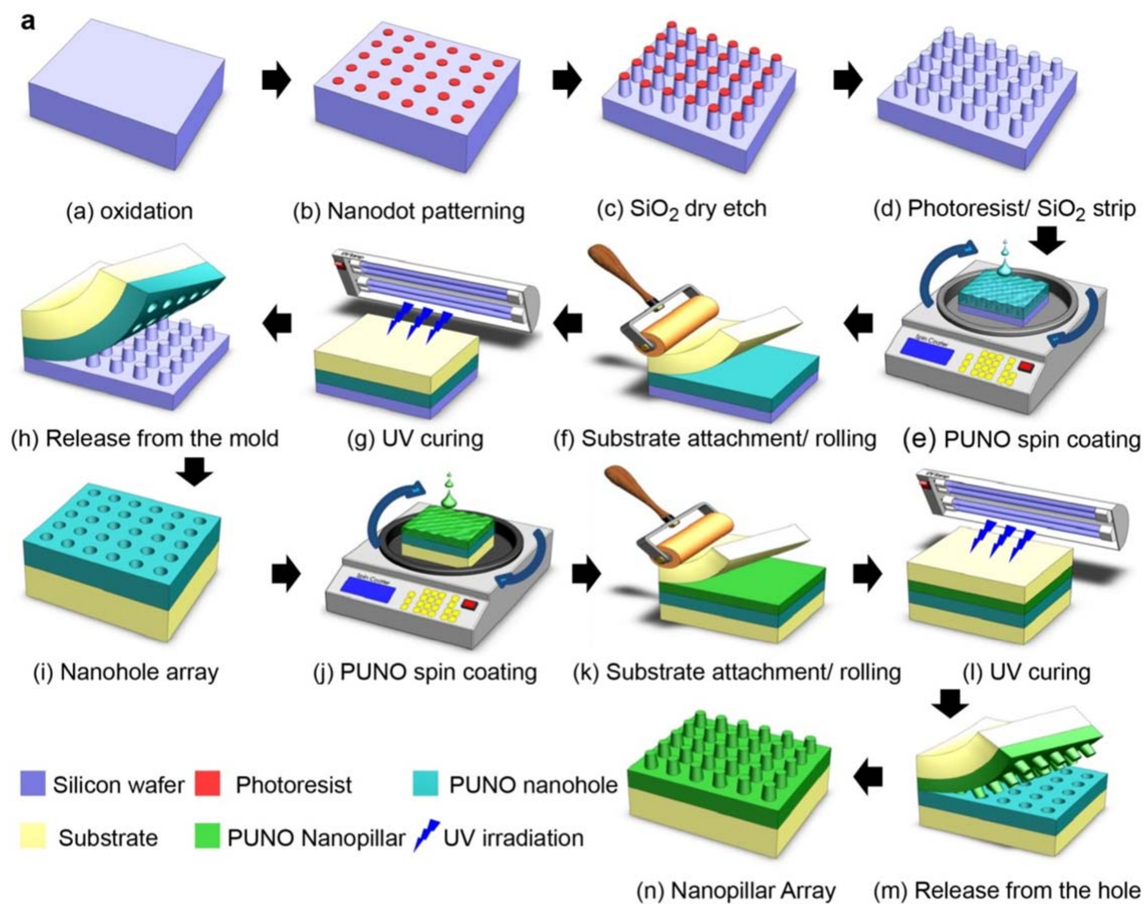

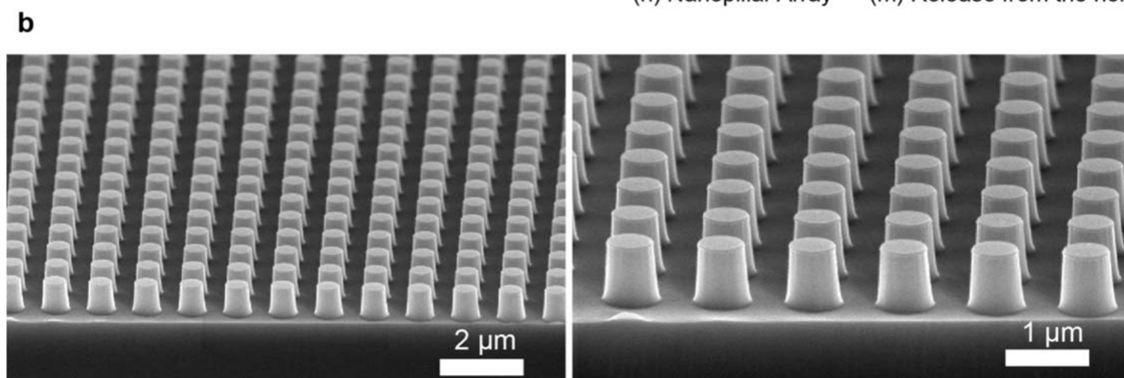

Figure S2. (a) Detailed schematic illustration for the polymeric nanopillar array fabrication process. (b) SEM images of the original Si nanopillar mold.

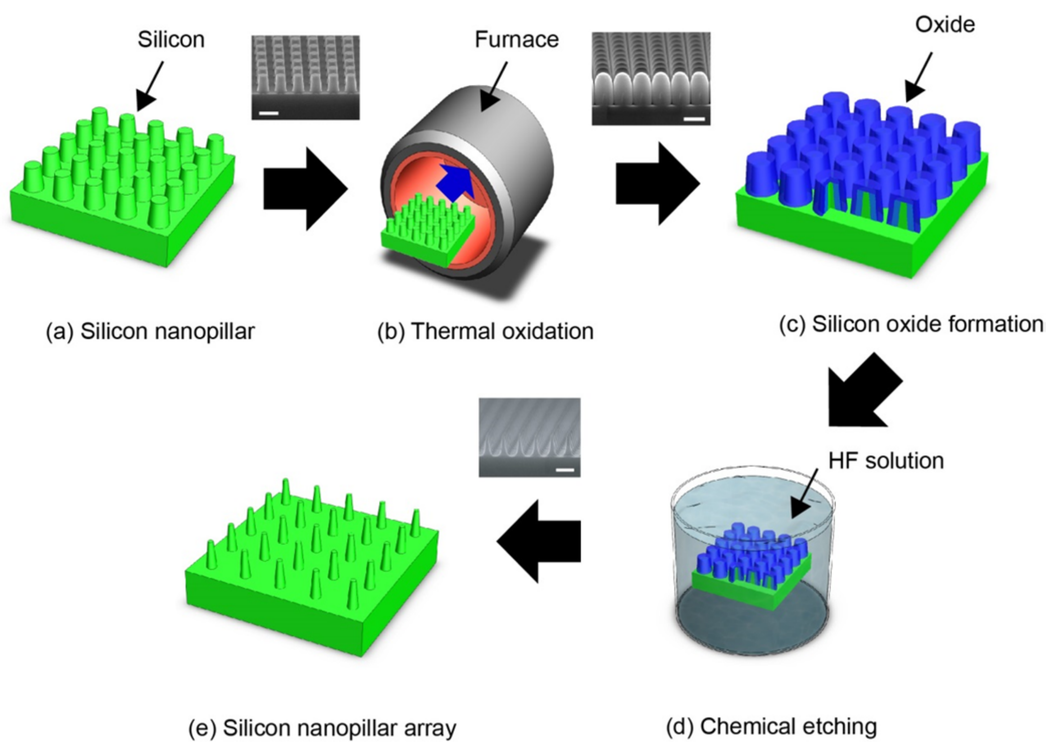

Figure S3. Schematic illustration of fabrication process of Si NPAs on a Si wafer.

The amount of oxygen doping to Si wafer converts Si into SiO_2 and determines the final dimension of Si NPAs. The oxide formation can be calculated using the Deal-Grove model [S6].

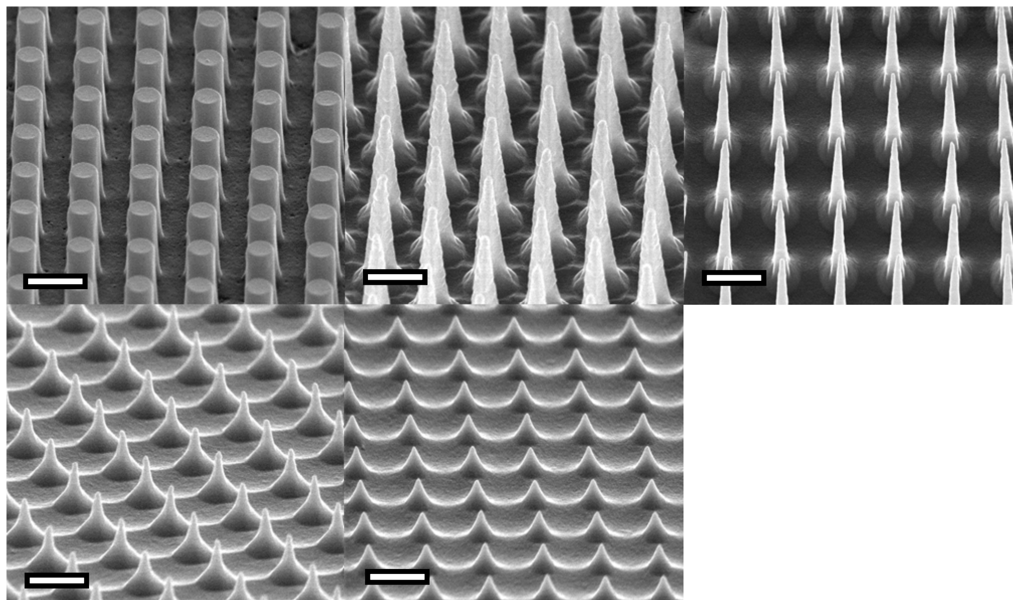

Figure S4. SEM images of NPAs under different oxidation conditions. Scale bars are 1 μm.

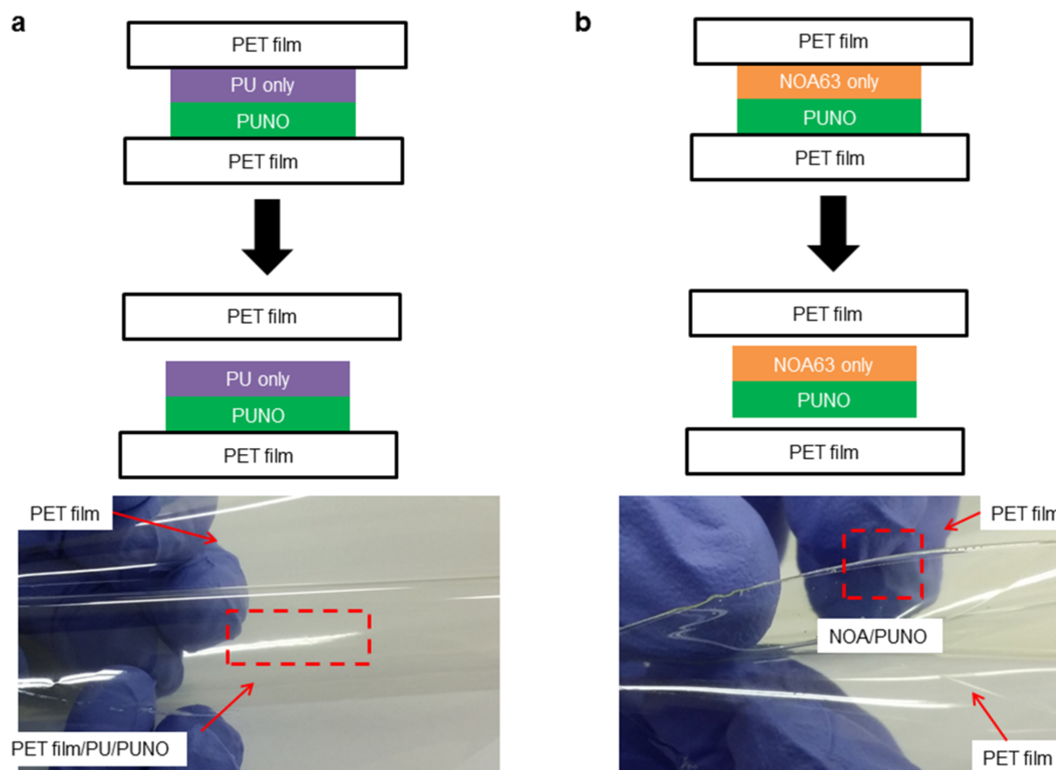

Figure S5. Adhesion test of (a) PU only and (b) NOA63 only to PUNO master mold.

The different ratio between NOA63 and PU were adopted for the adhesion to replicate the nanostructures from mold and target substrates. PU itself shows poor adhesion to PET film which makes impossible to release from mold. In case of NOA, its highly adhesive property demonstrates high bonding capability between NOA63/PUNO. Because of this strong adhesion, both top and bottom PET film were detached from NOA63/PUNO which is also impossible to replicate the structures from mold. Therefore, mixing ratio between NOA63 and PU can produce nanostructures from the mold.

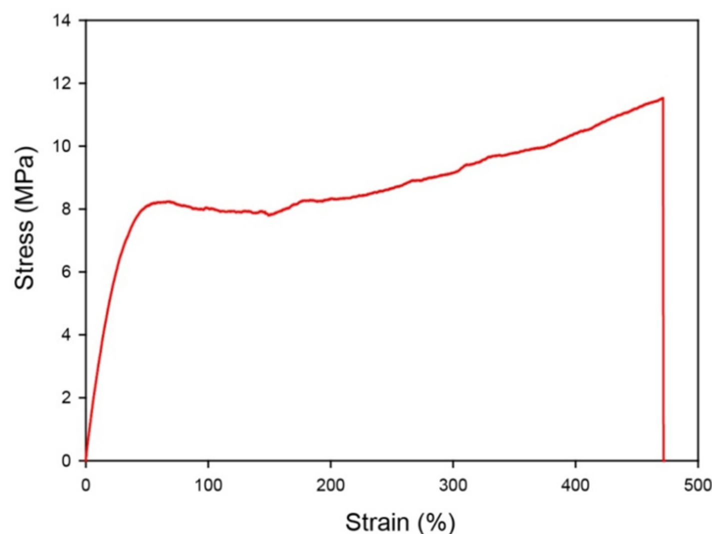

Figure S6. Stress – strain curve of PUNO thin film.

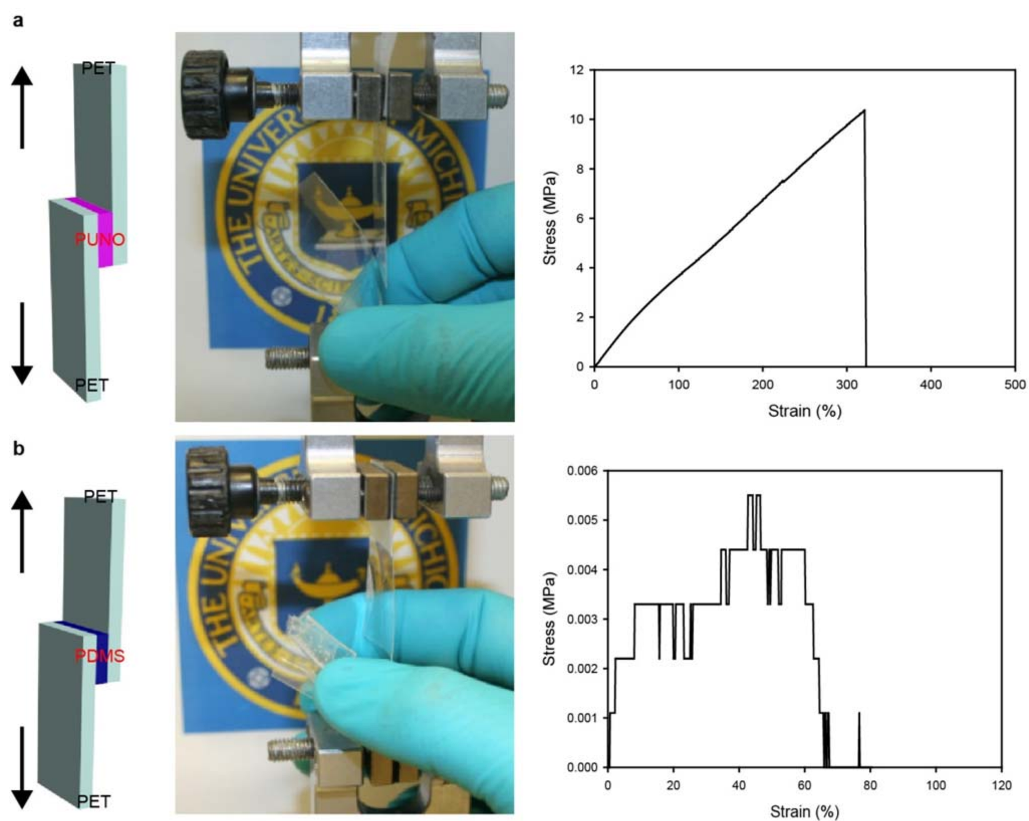

Figure S7. Adhesion tests for PET/PUNO/PET, PET/PDMS/PET, and fabric/PUNO/fabric test samples. Schematics and photographic images of the samples used in testing of adhesive characteristics of PUNO (a) and PDMS (b) placed between PET films under tensile force.

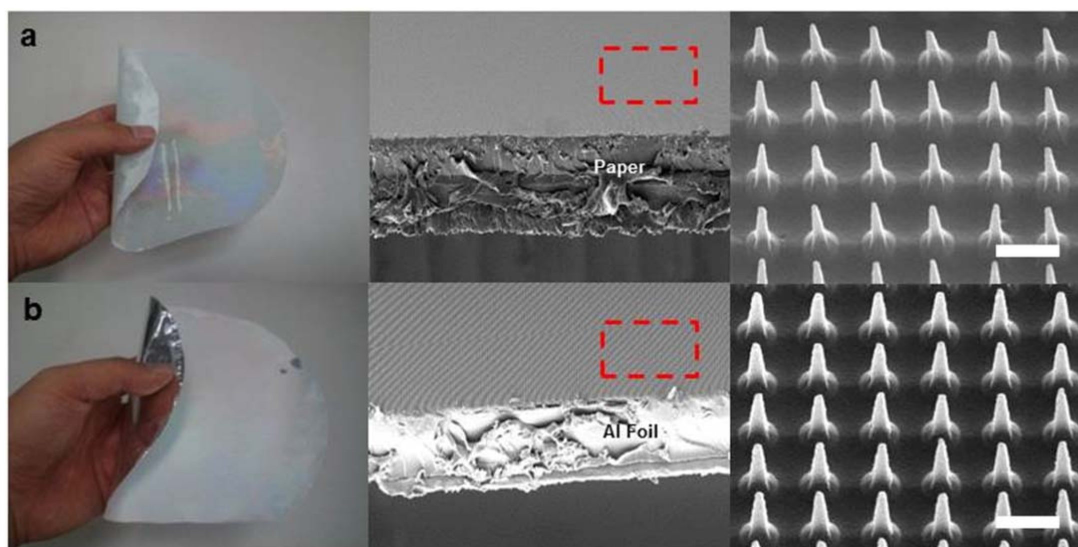

Figure S8. Photographic and SEM images of NPAs on paper (a) and Al foil (b), respectively. Scale bars are 1 μm

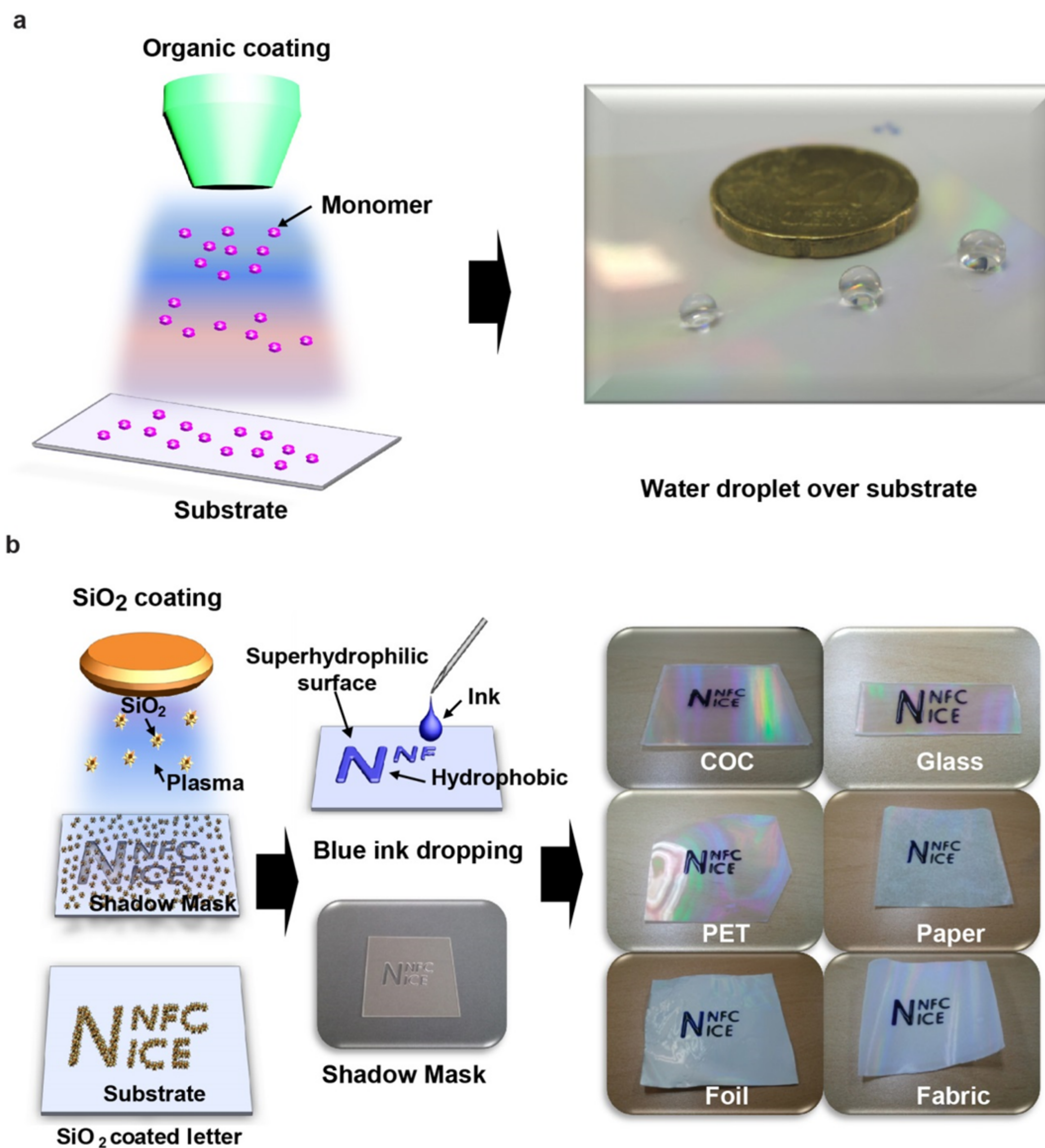

Figure S9. Schematic illustration of both superhydrophobic and superhydrophilic coating process and changing of their surface CAs . (a) NPAs surface conversion into superhydrophobic state. (b) Localized superhydrophilic coating over NPAs induce water ink pattern formation and present letters on the surface.

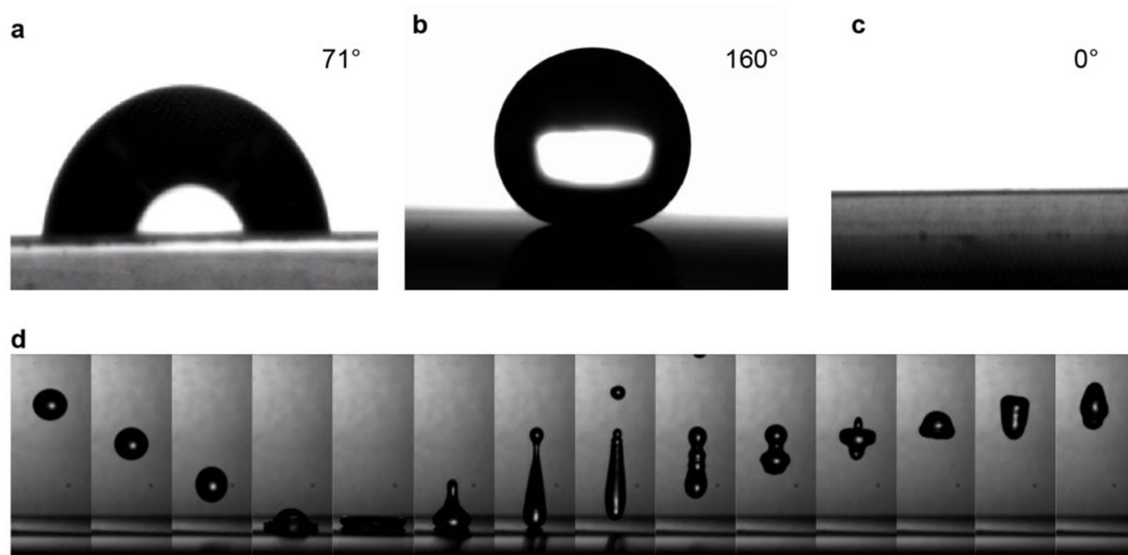

Figure S10. Photographic images of water droplet over pristine PUNO NPAs (a), after superhydrophobic (b) and superhydrophilic coating (c). (d) The corresponding water droplet bouncing over superhydrophobic surface snapshots from a high-speed camera (Supporting Video S1).

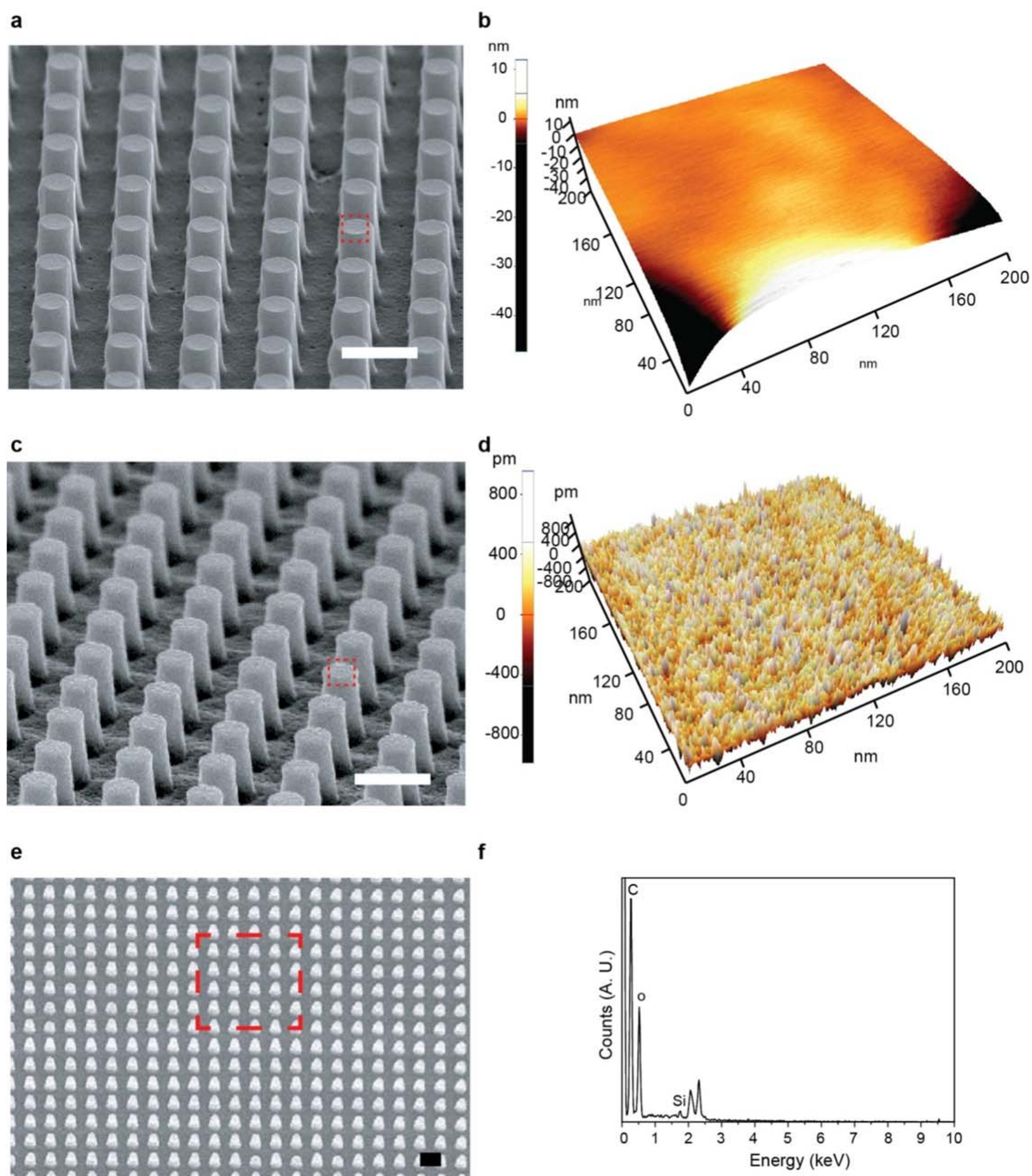

Figure 11. Surface roughness change over oxide coating over PUNO surface. SEM and AFM roughness images of polymeric nanopillars before SiO_2 coating (a,b) and after SiO_2 coating (c,d). SEM images of SiO_2-coated nanopillars arrays (e) and its energy dispersive X-ray spectra (f). Scale bars of SEM images are 1 μm.

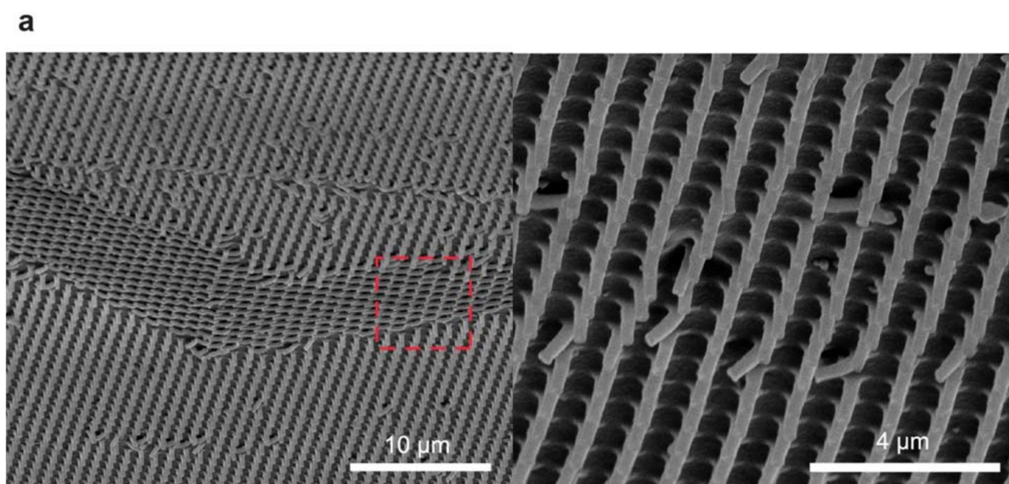

Figure S12. (a) The different magnifications of SEM images for NPAs after rubbing with finger.

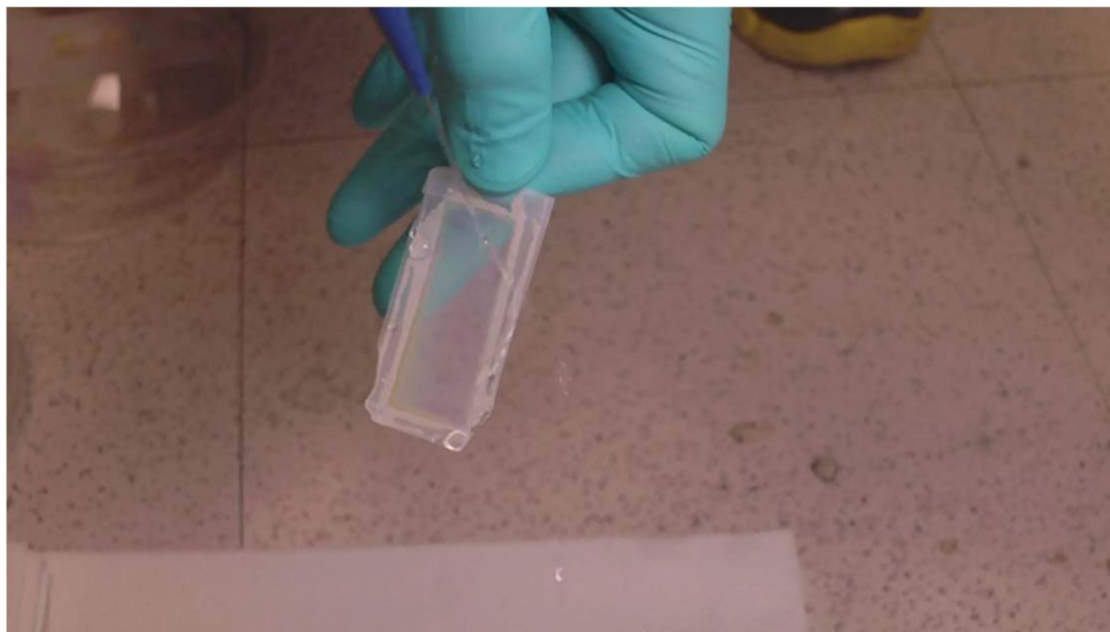

Supplementary Movie S1. Video clip (uploaded as a separate file) for the real time monitoring of the hydrophobic characteristic change after rubbing the NPA more than 500 times using fabric.

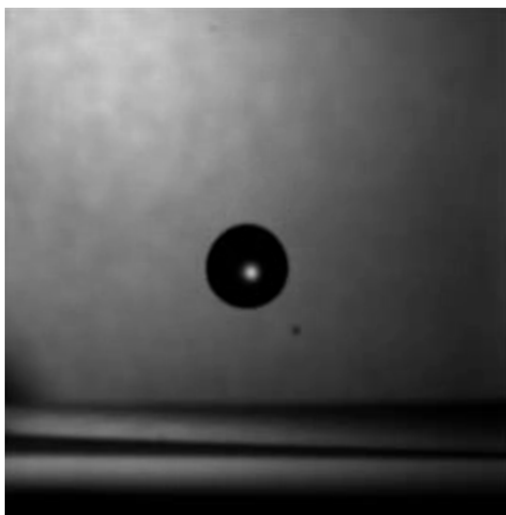

Supplementary Movie S2. Video clip for the real-time monitoring of the continuous bouncing forces of a water microdroplet against a superhydrophobic NPA for a period of ~71 sec using high speed camera.

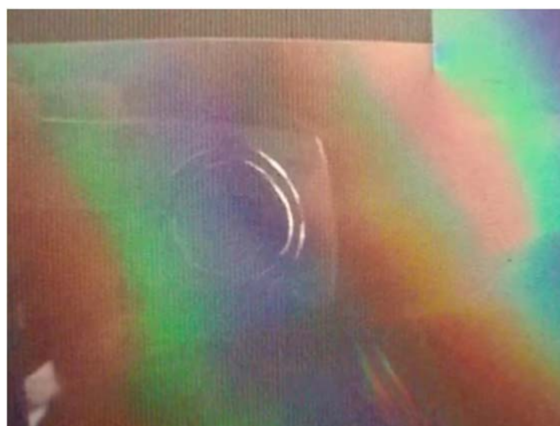

Supplementary Movie S3. Video clip for the real-time monitoring of the breath-activated images after inhaling and exhaling on the logo.

Supplementary References

S1. S.-J. Choi, H. N. Kim, W. G. Bae, K.-Y. Suh, *J. Mater. Chem.* **2011**, *21*, 14325.

S2. B. H. Kim, K. G. Lee, T. J. Park, H. Kim, T. J. Lee, S. J. Lee, D. Y. Jeong, *Small* **2012**, *8*, 3257.

S3. W. Lang, *Mater. Sci. Eng., R,* **1996**, *17*, 1.

S4. B. E. Deal, A. S. Grove, *J Appl Phys* **1965**, *36*, 3770.

S5. C. M. Andres, N. A. Kotov, *J. Am. Chem. Soc.* **2010**, *132*, 14496.

S6. S. Bhattacharya, A. Datta, J. M.Berg, S. Gangopadhyay. *J. Microelectromech. S.* **2005**, *14*, 590.

S7. J. B. You, K. I. Min, B. Lee, D. P. Kim, S. G. Im, *Lab Chip* **2013**, *13*, 1266.